Electronic Supplementary Information for

^{1}H and ^{13}C Chemical Shift–Structure Effects in Anhydrous β-Caffeine and Four Caffeine–Diacid Cocrystals Probed by Solid-State NMR Experiments and DFT Calculations

Debashis Majhi[†], Baltzar Stevensson, Tra Mi Nguyen, and Mattias Edén[*]

Department of Materials and Environmental Chemistry, Stockholm University,
SE-106 91 Stockholm, Sweden.
[†]Present address: Department of Chemistry, National Institute of Technology Tiruchirappalli,
Tiruchirappalli-620015, TamilNadu, India

[*]Corresponding author. E-mail: *mattias.eden@mmk.su.se*

Contents

S1 Aliphatic ^{1}H Chemical-Shift Changes Upon Cocrystal Formation

Both the experimental and modeled ^{1}H chemical shifts listed in Tables **3** and **4** reveal that the aliphatic C^1**H**$_2$/C^1**H** sites of the diacid moieties shield slightly by up to 1 ppm when the cocrystal is formed (i.e., $|\Delta^j_{\rm H}| \lesssim 1$ ppm). Despite the necessity of resorting to "aggregate" ($\overline{\delta}^j_{\rm H}$) values over 2–3 distinct CH$_n$ groups (*vide supra*), the excellent agreement between the $\overline{\delta}^j_{\rm H}$ NMR and GIPAW derived shifts of Table **3** suggest accurately modeled $\{\delta^j_{\rm H}\}$ values. For instance, from Figs. **5**d and **6**d readily assessed $\Delta_{\rm H}^{20/21}$ value accords very well with the GIPAW prediction, as do the "aggregate $\Delta_{\rm H}$ value" of the three methylene groups (H15–H17) of GA.

We onwards focus on the caffeine-stemming ^{1}H chemical shifts, namely the H4 and methyl (H6–H8) protons. As for the aliphatic ^{1}H sites of the diacids, the DFT/GIPAW calculations reproduce the experimental chemical shifts well (Table **3**) but are typically *lower* by $\lesssim 1$ ppm (except for $\delta^4_{\rm H}$). Although the total ^{1}H NMR-peak overlap among the three C^1**H**$_3$ sites of β-caffeine (Fig. **6**e) restricts the possibilities to gauge the chemical-shift alteration upon cocrystal formation, the markedly better ^{1}H NMR spectral resolution from the cocrystals (Fig. **6**) enables separate $\delta^6_{\rm H}$ assessments along with the average/CG chemical shift of C7^1**H**$_3$/C8^1**H**$_3$: both NMR and GIPAW suggest very similar $\delta^6_{\rm H}$ and $\overline{\delta}^{7/8}_{\rm H}$ values throughout all four cocrystals, *despite* variable HB and TB distances; see Fig. **2** and section **4.7**. This trend translates into a net CG chemical-shift difference of $\Delta_{\rm H} \approx 0$ ppm for the C^1**H**$_3$ groups relative to β-caffeine (Table **S3**), as reproduced by the GIPAW calculations within a minor and near-constant shift displacement ($\Delta_{\rm H} \approx 1$ ppm).

Likewise, the C4^1**H** chemical shift alters only marginally among the various cocrystals, as well as relative to that of β-caffeine. The remarkably small ^{1}H4 chemical-shift changes—which are observed *both* by NMR and GIPAW calculations—are attributed to the extensive H-bond formation in *both* β-caffeine and all cocrystals, each involving a C4**H**$\cdots$**O** HB (Fig. **2**), where the five distinct H4 sites of β-caffeine reveal a range of HB distances to neighboring molecules (section **4.2**). Moreover, *despite* that the C4**H**$\cdots$**O** distance varies between 216 pm in C-GA and 265 pm in C-ME among the cocrystals, a very modest deshielding degree is observed for the cocrystals ($\Delta^j_{\rm H} \approx 0.5$ ppm), whereas the DFT-derived counterparts are *even negative* of 1–2 ppm (Table **4**).

Table S1. Unit-Cell Parameters by Pawley Fitting of XRD Data[a]

Phase	Cell lengths (Å)			Cell angles (degrees)			Space Group	CCDC[b]	Ref.
	a	b	c	α	β	γ			
β-Caffeine	42.9556	15.0389	6.9384	90.0000	99.0546	90.0000	Cc		this work
	43.0390	15.0676	6.9531	90.0000	99.0274	90.0000	Cc	610381	S1
α-OA	6.5567	6.0939	7.8513	90.0000	90.0000	90.0000	$Pbca$		this work
	6.5678	6.0983	7.8715	90.0000	90.0000	90.0000	$Pbca$	1854356	S2
α-OA·2H_2O	6.1076	3.6096	12.1119	90.0000	106.2771	90.0000	$P2_1/n$		this work
	6.1169	3.6053	12.0490	90.0000	106.3030	90.0000	$P2_1/n$	703783	S3
β-MA	5.1573	5.3420	8.4052	108.5191	100.6892	94.9623	$P\bar{1}$		this work
	5.1582	5.3401	8.4024	108.4860	100.7120	94.9500	$P\bar{1}$	929777	S4
β-GA	12.9062	4.8234	9.9535	90.0000	96.8570	90.0000	$C2/c$		this work
	12.9680	4.8296	9.9820	90.0000	96.8720	90.0000	$C2/c$	1169312	S5
I-ME	7.6394	10.1149	7.6392	90.0000	119.3036	90.0000	$P2_1/c$		this work
	7.1511	10.1107	7.6405	90.0000	119.4050	90.0000	$P2_1/c$	1435260	S6
2C–OA	4.4361	14.8522	16.0758	90.0000	97.4556	90.0000	$P2_1/c$		this work
	4.4143	14.7701	15.9119	90.0000	96.4850	90.0000	$P2_1/c$	272620	S7
2C–MA	30.5951	31.3857	4.7008	90.0000	90.0000	90.0000	$Fdd2$		this work
	30.3992	31.2845	4.6739	90.0000	90.0000	90.0000	$Fdd2$	272621	S7
C–GA	8.3651	8.6844	11.4829	69.3951	77.9667	74.7729	$P\bar{1}$		this work
	8.3212	8.6667	11.3636	68.9550	78.5590	74.2360	$P\bar{1}$	229593	S7
C–ME	7.0312	12.5188	15.8410	90.0000	93.2495	90.0000	$P2_1/n$		this work
	6.8565	12.5051	15.8362	90.0000	93.6100	90.0000	$P2_1/n$	272622	S7

[a] Unit cell parameters obtained by Pawley fitting of the PXRD data of Figs. **S1** and **S2** by using the TOPAS software[S8] (first line of each entry), along with the input parameters reported previously (second line) by the as-stated source (rightmost column).
[b] Deposition number in the Cambridge crystallographic data center.

Table S2. Cell Parameters in DFT Calculations[a]

Phase	Cell lengths (Å)			Cell angles (degrees)			Space Group	CCDC[b]	Ref.
	a	b	c	α	β	γ			
β-Caffeine	22.8002	22.8002	6.9531	98.5165	98.5165	38.5894	$P1$	610381	S1
	22.3089	22.3089	6.4195	102.0568	102.0568	37.8282	$P1$		this work
α-OA	6.5678	6.0983	7.8715	90.0000	90.0000	90.0000	$Pbca$	1854356	S2
α-OA·2H_2O	6.1169	3.6053	14.9658	90.0000	129.4000	90.0000	$P2_1/c$	703783	S3
β-MA	5.1582	5.3401	8.4024	108.4860	100.7120	94.9500	$P\bar{1}$	929777	S4
β-GA	12.9769	4.7484	9.6955	90.0000	98.3000	90.0000	$C2/c$	1169311	S5
	12.7258	4.4911	9.2097	90.0000	99.4700	90.0000	$C2/c$		this work
I-ME	7.1511	10.1107	7.6405	90.0000	119.4050	90.0000	$P2_1/c$	1435260	S6
	6.5778	9.7388	7.0958	90.0000	116.2407	90.0000	$P2_1/c$		this work
2C–OA	4.4143	14.7701	15.9119	90.0000	96.4850	90.0000	$P2_1/c$	272620	S7
2C–MA	30.3992	31.2845	4.6739	90.0000	90.0000	90.0000	$Fdd2$	272621	S7
C–GA	8.3212	8.6667	11.3636	68.9550	78.5590	74.2360	$P\bar{1}$	229593	S7
	7.9625	8.4191	10.9214	68.4349	79.9799	73.5924	$P\bar{1}$		this work
C–ME	6.8565	12.5051	17.6485	90.0000	116.4200	90.0000	$P2_1/c$	272622	S7
	6.3348	12.2965	17.0267	90.0000	115.1100	90.0000	$P2_1/c$		this work

a Unit cell parameters (from the as-indicated source) as input to the CASTEP software after conversion of the parameters listed in Table **S1** by the CIF2Cell program (version 1.2.10).[S9] The $^1H/^{13}C$ chemical shifts reported herein were obtained by an initial energy optimization by DFT, during which only the H atom positions were adjusted. For the {β-caffeine, β-GA, I-ME, C–GA, C–ME} structures, an additional DFT optimization was performed, where all cell parameters *and* atom positions were adjusted freely, giving the refined {a, b, c} and {α, β, γ} values listed as "this work". However, except for β-caffeine, that gave no improvements relative to experiments; see section **4.3**.

b Deposition number in the Cambridge crystallographic data center.

Table S3. $^{13}\mathbf{CH}_3$ **Chemical Shifts and HB/TB-Distance Information**[a]

	2C–OA	2C–MA	C–GA	C–ME	β-Caffeine[b]	Site
C6H$_3$						
NMR: δ_C^6; Δ_C^6 (ppm)	36.5; 1.4	34.0; −1.0	34.3; −0.7	36.5; 1.5		
DFT: δ_C^6; Δ_C^6 (ppm)	36.2; 0.9	33.0; −2.3	33.5; −1.7	36.6; 1.4		
HB: C**H**$_3\cdots$O (pm)	223(O1)	241(O2)	234(O1)	249(O19H)	207; 240; 259	O2
	292(O2)	292(O1)	236(O18)	259(O2)	234; 276	O1
			278(O14H)	267(O22)		
TB: **C**H$_3\cdots$O (pm)	323(O1)	342(O2)	337(O18)	333(O22)	291; 294; 312	O2
	325(O2)	369(O1)	343(O1)	337(O2)	301; 301	O1
	354(O1)		371(O14H)	349(O22)		
C7H$_3$						
NMR: δ_C^7; Δ_C^7 (ppm)	31.1; 0.4	31.6; 0.9	31.5; 0.8	31.4; 0.7		
DFT: δ_C^7; Δ_C^7 (ppm)	28.5; −1.1	30.0; 0.3	29.1; −0.6	29.7; 0.0		
HB: C**H**$_3\cdots$O/N (pm)	255(O1)	261(O1)	272(O14H)	257(O22)	252; 264	N
	260(O9H)	269(O11H)	272(O1)	260(O19H)	271; 296	O1
	292(O1)	280(O2)	278(O18)	265(O22H)	281	O2
		327(O11H)	305(O1)	266(O22)		
				290(O22)		
TB: **C**H$_3\cdots$O/N (pm)	329(O1)	304(O1)	347(O1)	340(O22)	338; 346	N
	337(O9H)	353(O11H)	354(O18)	342(O19H)	345	O2
	349(O2)	353(O2)	356(O1)	356(O19H)	363; 392	O1
			362(O14H)	356(O22)		
C8H$_3$						
NMR: δ_C^8; Δ_C^8 (ppm)	27.9; −1.7	28.3; −1.3	27.8; −1.8	29.0; −0.7		
DFT: δ_C^8; Δ_C^8 (ppm)	25.2; −4.3	25.8; −3.7	24.2; −5.3	27.4; −2.0		
HB: C**H**$_3\cdots$O/N (pm)	272(O9H)	245(O11)	255(O18H)	266(O19)	236; 266	O2
	285(O9)	262(O11)	339(O14)	272(O2)	258; 281	O1
				286(O19)	294	N
TB: **C**H$_3\cdots$O/N (pm)	339(O9)	312(O11)	321(O18H)	315(O22H)	318; 341	O2
	340(O9H)	343(O11)	354(O18H)	354(O19)	326; 353	O1
					340	N

[a] A compilation of the methyl-group-associated ^{13}C chemical shifts $\{\delta_C^6, \delta_C^7, \delta_C^8\}$ of the caffeine-moiety in the cocrystals and their Δ_C^j counterparts relative to β-caffeine [eqn (6)], as deduced from either ^{13}C NMR experiments or DFT/GIPAW calculations. The chemical shifts are contrasted with the DFT-derived set of shortest HB (C**H**$_3\cdots$O) and TB (**C**H$_3\cdots$O) distances in each cocrystal (and thereby most influential on δ_C^j/Δ_C^j; see Fig. **2**), listed with increasing distance from top to bottom. Note that for graphical visualization limitations, some of the shortest distances are not indicated in Fig. **2**.

[b] The shortest HB/TB distances encountered for the five crystallographically unique caffeine sites/molecules of the DFT-refined structure along with the identity of the O1/O2/N atom involved in the bond (specified in the rightmost column). Note that *all five* HB/TB distances listed for β-caffeine contribute to each respective ^{13}C6–^{13}C8 chemical shift, as opposed to the distance counterparts of the cocrystals that involve multiple distances from *one* unique ^{13}C site, whose impact on its chemical shift decreases drastically for increasing HB/TB distance.

Table S4. Experimental ^{13}C FWHM Values Determined by MAS NMR[a]

		Coformer	2C–OA	2C–MA	C–GA	C–ME
		fwhm	fwhm	fwhm	fwhm	fwhm
Coformer	Site	(ppm)	(ppm)	(ppm)	(ppm)	(ppm)
β-Caffeine	C1	1.90	0.72	0.38	0.80	1.07
	C2	n.d.	0.84	0.56	0.91	1.14
	C3	n.d.	0.81	0.49	0.86	1.16
	C4	2.88	0.83	0.42	0.90	1.16
	C5	1.33	0.75	0.43	0.83	1.08
	C6	2.36	0.78	0.36	0.89	1.10
	C7	n.d.	0.79	0.42	1.01	1.16
	C8	n.d.	0.81	0.41	0.84	1.17
α-OA	C9/10	0.61	0.73			
α-OA·2H_2O	C9/10	0.68	0.73			
β-MA	C11	0.19		0.30		
	C12	0.21		0.22		
	C13	0.19		0.30		
β-GA	C14	0.59			0.79	
	C15	0.81			1.10	
	C16	0.89			1.09	
	C17	0.81			n.d.	
	C18	0.59			0.78	
I-ME	C19	1.60				1.06
	C20	1.58				1.13
	C21	1.53				1.12
	C22	1.58				1.04

[a] FWHM (within ±0.05 ppm) of each ^{13}C NMR peak observed in the spectra from the cocrystals and their precursor phases. Only data for sufficiently resolved resonances are listed.

Table S5. DFT-Derived ^{1}H Chemical Shifts[a]

		Coformer	2C–OA	2C–MA	C–GA	C–ME
Coformer	Site	δ_H/ppm	δ_H/ppm	δ_H/ppm	δ_H/ppm	δ_H/ppm
β-caffeine	H4	8.4	7.2	7.6	7.3	6.7
	H6	4.5	3.7	3.8	3.5	3.2
	H7	3.6	2.5	2.8	2.4	2.6
	H8	3.5	1.8	1.8	2.2	2.0
α-OA	HO9/10	11.2	15.0			
α-OA·2H_2O	HO9/10	17.8	15.0			
	H_2O	5.1/6.0				
β-MA	HO11	13.7		14.8		
	H12a	2.7		1.7		
	H12b	2.5		1.7		
	HO13	13.4		14.8		
β-GA	HO14	13.7			14.0	
	H15a	1.6			1.4	
	H15b	1.2			1.5	
	H16a	0.2			0.3	
	H16b	0.2			0.4	
	H17a	1.6			0.9	
	H17b	1.2			1.7	
	HO18	13.7			10.6	
I-ME	HO19	13.6				20.2
	H20	6.1				4.8
	H21	6.3				4.9
	HO22	16.2				14.6

[a] The entire set of DFT/GIPAW-derived ^{1}H chemical shifts from the unique $^1\mathbf{H}j$ site of each sample.

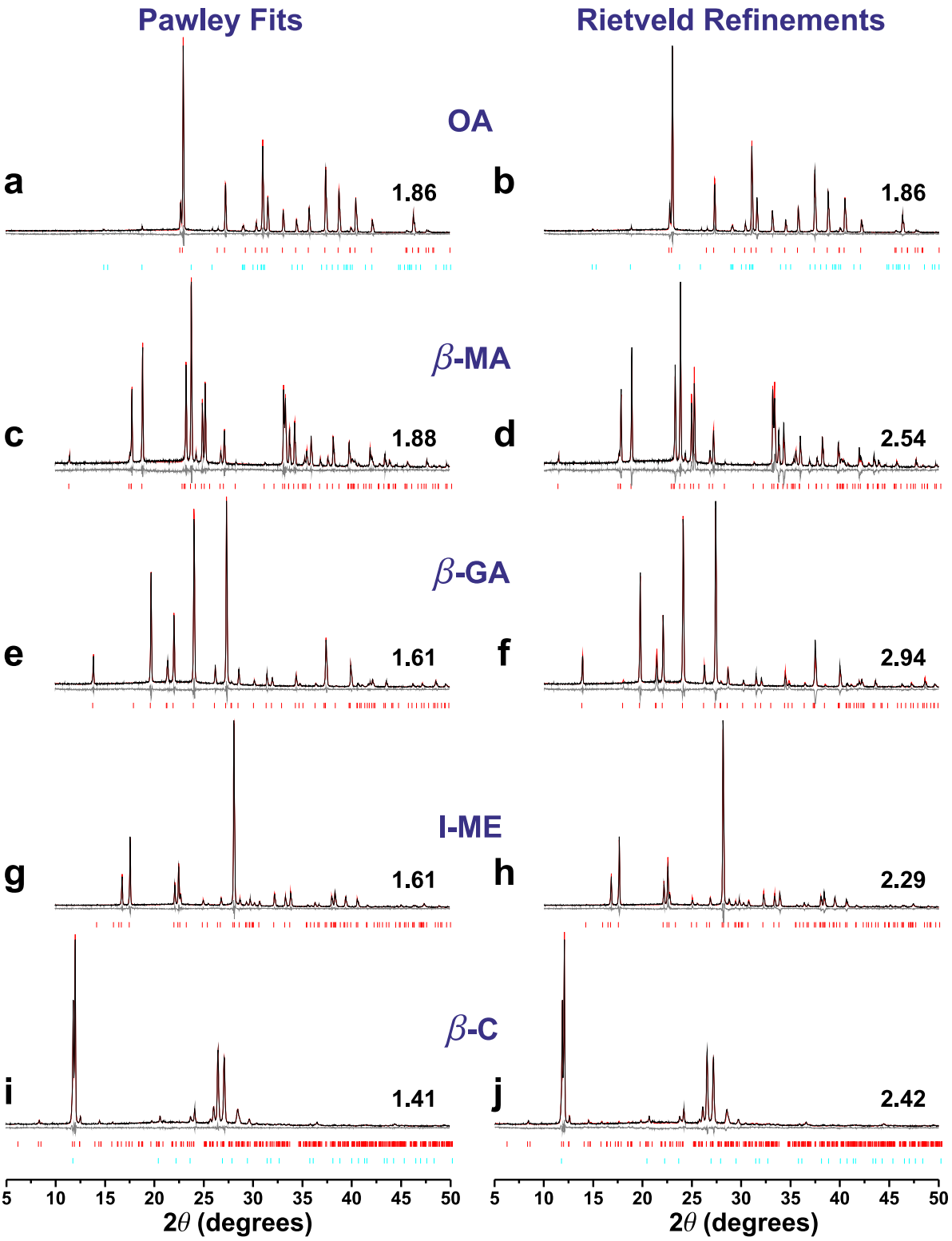

Fig. S1. Powder diffractograms (black traces) and best-fit results (red traces) by Pawley (left column) and Rietveld (right column) analyses for the cocrystal precursors of (a, b) α-OA/α-OA·2H$_2$O mixture ("OA"), (c, d) malonic acid (β-MA), (e, f) glutaric acid (β-GA), (g, h) maleic acid (I-ME), and (i, j) anhydrous β-caffeine (β-C), for the structures presented in Table **S1**. Each number at the right diffractogram portion specifies the "goodness-of-fit",[S8] while the grey curve beneath each PXRD pattern represents the difference between the experiment and best fit. The red and cyan Bragg-peak markers in (a, b) correspond to the peak positions from the α-OA and α-OA·2H$_2$O phases, respectively, whereas those in (i, j) mark the peaks from anhydrous β-caffeine (red; Table **S1**) and α-caffeine (cyan; space group $R\bar{3}c$; CCDC 274185[S10]).

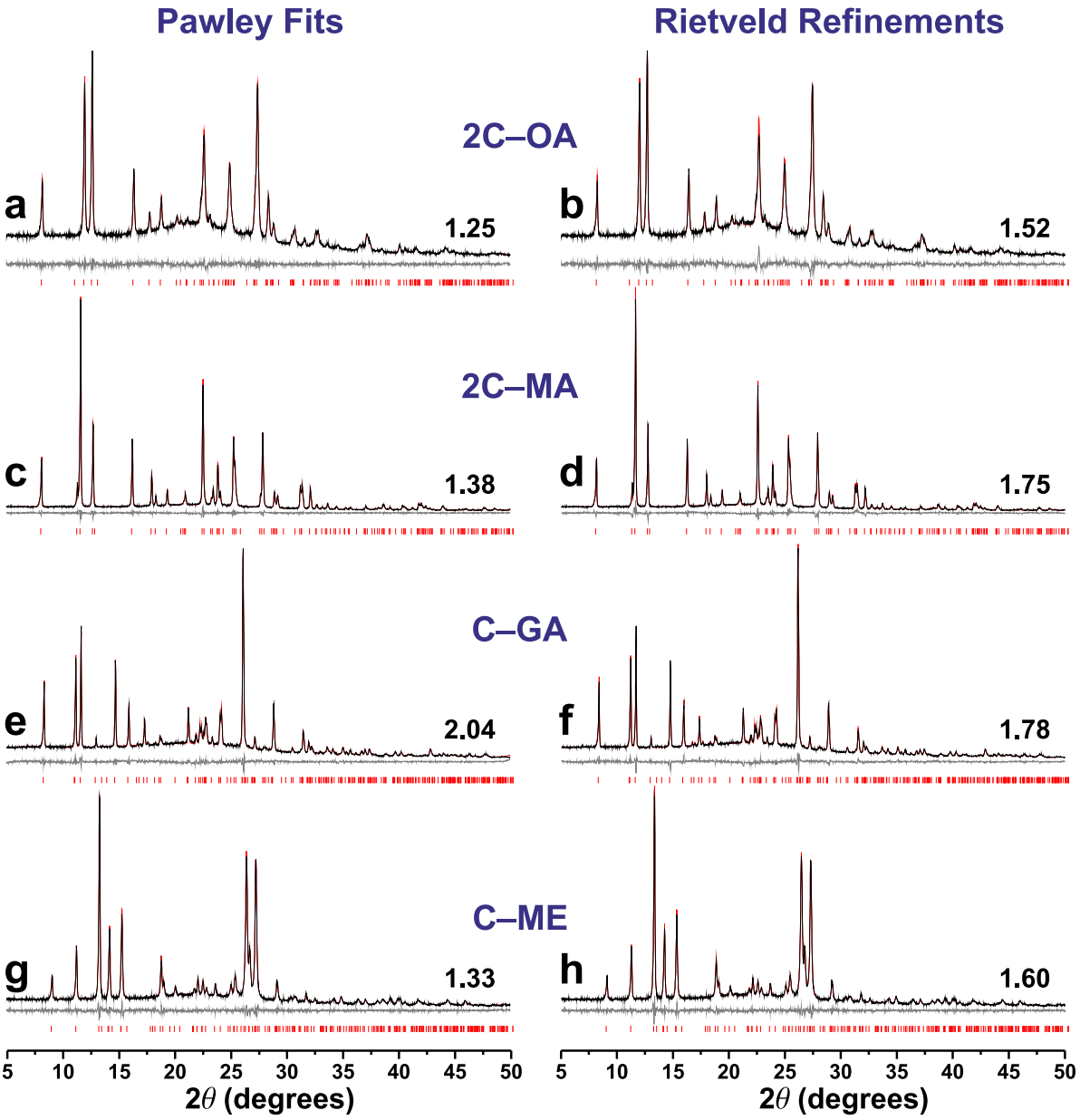

Fig. S2. Powder diffractograms (black traces) and best-fit results (red traces) by the Pawley (left column) and Rietveld (right column) methods for the (a, b) 2C–OA, (c, d) 2C–MA, (e, f) C–GA, (g, h) C–ME cocrystals (see Table **S1**). Each number at the right diffractogram portion specifies the "goodness-of-fit",[S8] while the grey curve beneath each PXRD pattern represents the difference between the experiment and best fit.

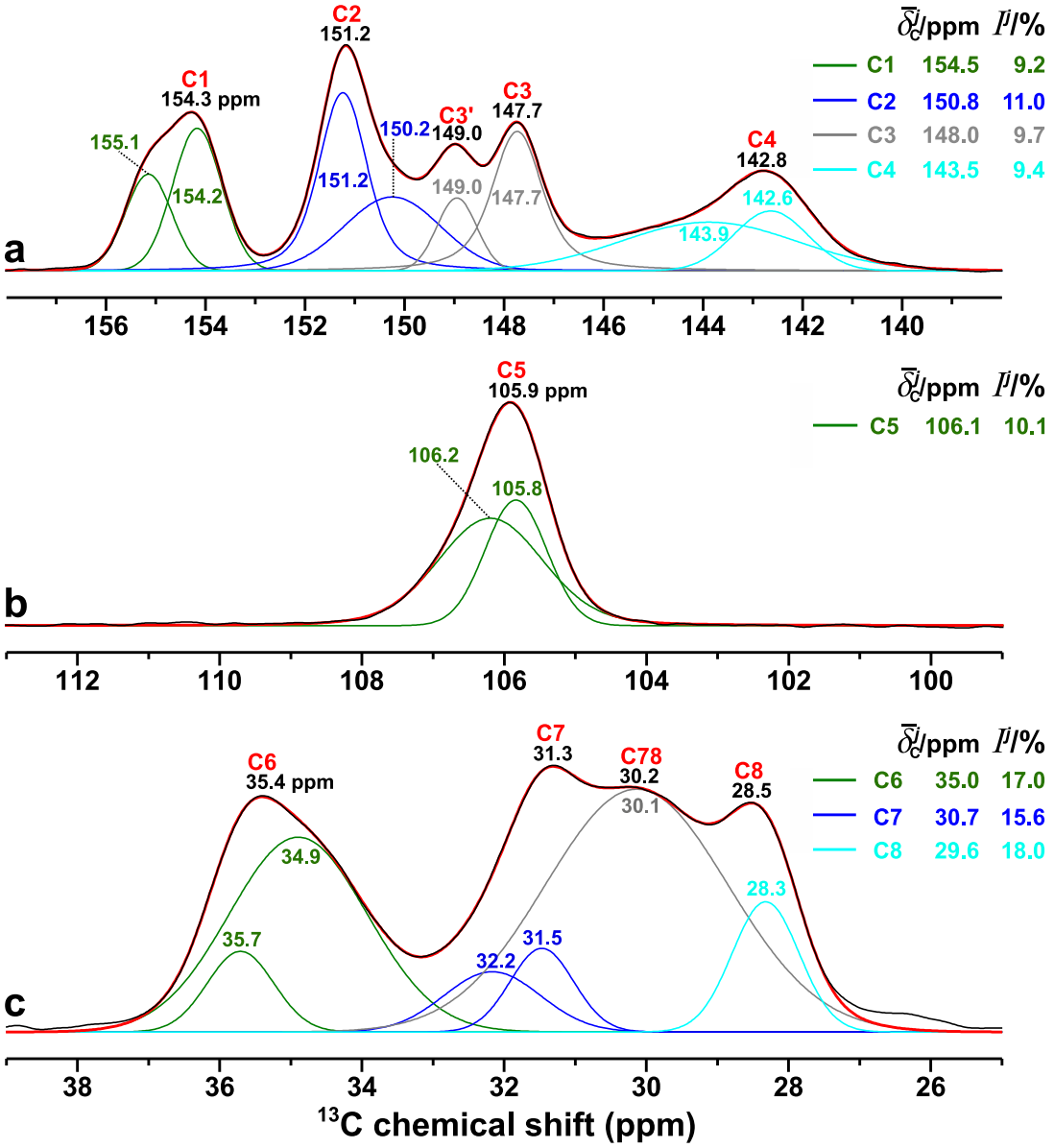

Fig. S3. Experimental ^{13}C MAS NMR spectrum (black traces) of anhydrous β-caffeine (Fig. **3**e), shown together with its best-fit result (red traces) and deconvolutions into component peaks stemming from the eight distinct ^{13}C sites (C1–C8), where all NMR peaks associated with a given site are presented with the same color (see legends). All numbers (in ppm) above each ^{13}C peak represents its chemical shift at the peak maximum. The legends list each center-of-gravity shift ($\bar{\delta}_{\rm C}^{j}$) together with its associated fraction (I^{j}) contributed by site ^{13}Cj (out of the total spectral intensity), which was obtained by the sum over all its peak components. Note that panels (a–c) employ different vertical scales.

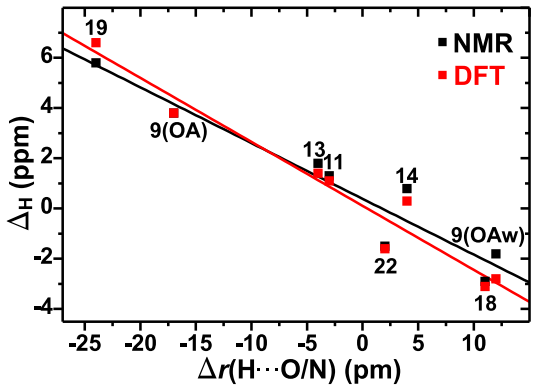

Fig. S4. Experimental (black symbols) and DFT-generated (red) ^{1}H chemical-shift differences [$\Delta^j_{\rm H}$; eqn (5)] plotted against the difference in HB distance, Δr(H$\cdots$O/N), between the carboxy moieties of the cocrystal and its diacid precursor. The black and red lines are best-fit results, yielding the respective expressions $\Delta^j_{\rm H}$[NMR]/ppm$= 0.385 - 0.222\Delta r$(H$\cdots$O/N)/pm ($R^2 = 0.915$), and $\Delta^j_{\rm H}$[DFT]/ppm$= 0.107 - 0.255\Delta r$(H$\cdots$O/N)/pm ($R^2 = 0.943$).

References

(S1) C. W. Lehmann and F. Stowasser, The crystal structure of anhydrous β-caffeine as determined from X-ray powder-diffraction data, *Chem. Eur. J.*, 2007, **13**, 2908–2911.

(S2) S. Bhattacharya, Thermal expansion and dimensionality of a hydrogen bond network: a case study on dimorphic oxalic acid, *CrystEngComm*, 2020, **22**, 7896–7902.

(S3) N. Casati, P. Macchi, and A. Sironi, Hydrogen migration in oxalic acid di-hydrate at high pressure?, *Chem. Commun.*, 2009, pp. 2679–2681.

(S4) S. Bhattacharya, V. G. Saraswatula, and B. K. Saha, Thermal expansion in alkane diacids–another property showing alternation in an odd–even series, *Cryst. Growth Des.*, 2013, **13**, 3651–3656.

(S5) V. R. Thalladi, M. Nüsse, and R. Boese, The melting point alternation in α,ω-alkanedicarboxylic acids, *J. Am. Chem. Soc.*, 2000, **122**, 9227–9236.

(S6) D. Rychkov, S. Arkhipov, and E. Boldyreva, Structure-forming units of amino acid maleates. Case study of L-valinium hydrogen maleate, *Acta Cryst.*, 2016, **B72**, 160–163.

(S7) A. V. Trask, W. D. S. Motherwell, and W. Jones, Pharmaceutical cocrystallization: Engineering a remedy for caffeine hydration, *Cryst. Growth Des.*, 2005, **5**, 1013–1021.

(S8) A. Coelho, TOPAS-academic v6, *Coelho Software*, 2016.

(S9) T. Björkman, CIF2Cell: Generating geometries for electronic structure programs, *Comp. Phys. Commun.*, 2011, **182**, 1183–1186.

(S10) G. D. Enright, V. V. Terskikh, D. H. Brouwer, and J. A. Ripmeester, The structure of two anhydrous polymorphs of caffeine from single-crystal diffraction and ultrahigh-field solid-state ^{13}C NMR spectroscopy, *Cryst. Growth Des.*, 2007, **7**, 1406–1410.